Coordination Chemistry Reviews, 65 (1985) 141–165
Elsevier Science Publishers B.V., Amsterdam – Printed in The Netherlands

THE $A_2[FeX_5(H_2O)]$ SERIES OF ANTIFERROMAGNETS

RICHARD L. CARLIN

Department of Chemistry, University of Illinois at Chicago, Chicago, Illinois 60680 (U.S.A.)

FERNANDO PALACIO

Department of Thermodynamics, Faculty of Sciences, University of Zaragoza, 50009-Zaragoza (Spain)

(Received 23 October 1984)

CONTENTS

A. INTRODUCTION

It has long been known that one can easily prepare salts of the $[FeX_5(H_2O)]^{2-}$ anion (X = halide) from aqueous solutions. Slow evaporation of stoichiometric mixtures of metal chloride or bromide and the appropriate ferric halide in acidic solution yields crystals of the desired $A_2[FeX_5(H_2O)]$ salt (A = alkali metal or ammonium ion); only the monohydrate seems to grow under these conditions [1]. The clarity of the red/orange crystals, which are nicely suitable for spectroscopy [2], suggests that there is little hydrolysis of the hydrated iron(III) ion in the crystal. This simple preparative procedure stands in marked contrast to the difficulties involved in forming salts of the $[FeCl_6]^{3-}$ ion [3]. Although there are reports in the literature of compounds in the $[FeCl_{5-x}Br_x(H_2O)]^{2-}$ series, we have as yet been unable to prepare single crystals of any of these materials.

The substances of formula $A_2[FeX_5(H_2O)]$ have recently been found to

0010-8545/85/$08.75

undergo magnetic ordering at easily accessible temperatures. The compounds are antiferromagnets; an important point is that the exchange interactions are much stronger than is usually observed with hydrated double salts of the other transition metal ions. One reason for studying these compounds is that antiferromagnets of isoelectronic manganese(II) are much better known, in part because the syntheses are easier; so much has been learned from the study of the manganese salts that one hopes that further exploration of iron salts will be equally fruitful.

B. CRYSTALLOGRAPHY

All the compounds but one are orthorhombic although they are not isomorphic; the cesium compound $Cs_2[FeCl_5(H_2O)]$ belongs to the space group *Cmcm* [4,5] and is isomorphic to the analogous ruthenium(III) material [6]. The remaining compounds except for monoclinic [7] $K_2[FeF_5(H_2O)]$ belong to space group *Pnma* [1]. The available crystallographic results are summarized in Table 1, and a sketch of the structure of $Cs_2[FeCl_5(H_2O)]$ is presented in Fig. 1. The interesting isomorphous [8] compound $(H_3O)_2[FeCl_5(H_2O)]$ is included in the table for completeness, although there are as yet no magnetic measurements on this material. The substances $(NH_4)_2[FeCl_5(H_2O)]$ and $(NH_4)_2[InCl_5(H_2O)]$ are isomorphous [9,10], which is useful because the indium compound thus furnishes a colorless, diamagnetic analog. Even the analogous molybdenum(III) chloride and bromide salts are isomorphous [11]! The crystallographic similarities indicated are important because one parameter is thereby removed when the magnetic and other properties of these compounds are compared. All of the materials studied so far are antiferromagnets, and this is therefore one of the largest series of structurally-related antiferromagnets of a given metal ion available.

The crystals contain discrete $[FeX_5(H_2O)]^{2-}$ octahedra which are hydrogen-bonded together. There are four crystallographically equivalent molecules in a unit cell, arranged in two antiparallel pairs. The octahedra are always found to be slightly distorted, with the exact dimensions depending on the nature of the particular counterion. Several exhaustive discussions of the structures and the way they affect magnetic properties have appeared [12–14]. The essential feature is that there are no μ-bridging groups between the metal ions, such as an Fe–O–Fe or Fe–Cl–Fe linkage. All the superexchange paths are of the sort Fe–Cl---Cl–Fe, Fe–Cl---H–O(H)–Fe or variants thereof. In some cases there are two such paths between any two given metal ions. What is unusual is how well these relatively long paths transmit the superexchange interaction.

TABLE 1

Crystallographic properties of $A_2[FeX_5(H_2O)]$

A, X	Cs, Cl	Rb, Cl	K, Cl	NH_4, Cl	H_3O, Cl	Cs, Br	Rb, Br	K, F	$(NH_4)_2[InCl_5(H_2O)]$	$K_2[InCl_5(H_2O)]$
Space group	*Cmcm*	*Pnma*	*Pnma*	*Pnma*	*Pnma*	*Pnma*	*Pnma*	*C2/c*	*Pnma*	*Pnma*
a (Å)	7.442, 7.426	13.825	13.75	13.706	13.720	14.7	14.2	9.71	14.10	13.905
b (Å)	17.307, 17.306	9.918	9.92	9.924	9.926	10.7	10.4	7.79	10.17	9.952
c (Å)	8.077, 8.064	7.100	6.93	7.024	7.038	7.6	7.4	7.95	7.16	7.185
β (°)	–	–	–	–	–	–	–	96.5	–	–
Z	4	4	4	4	4	4	4	4	4	4
Ref.	4, 5	4	Quoted in 12	9	8	1	1	7	34	10

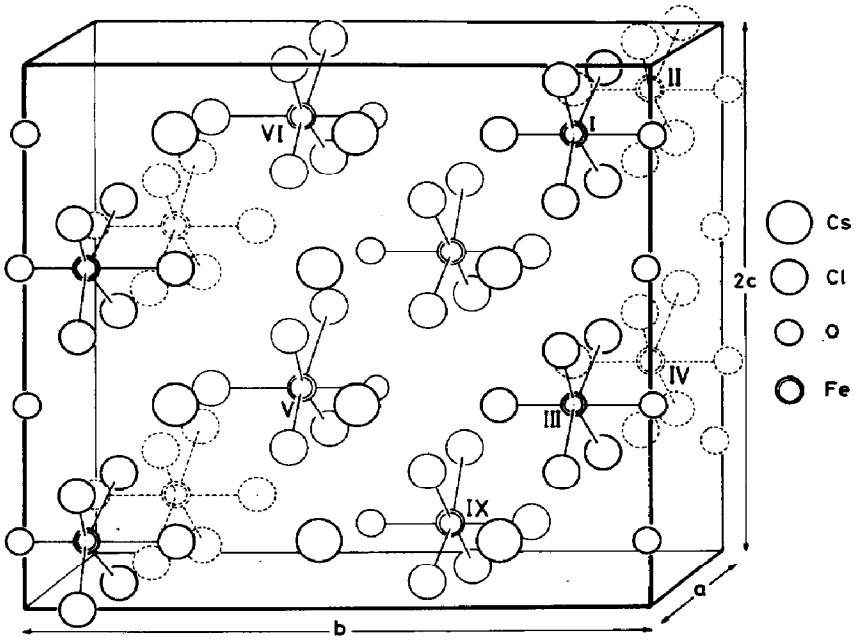

Fig. 1. Crystal structure of $Cs_2[FeCl_5(H_2O)]$. The unit cell is doubled along the *c* axis. For clarity, only the Cs atoms in the frontal *bc* plane have been included. The differences in thickness of the atoms indicate different *bc* planes. From ref. 13.

C. MAGNETOCHEMISTRY OF IRON(III)

The magnetochemistry of iron(III) is relatively straightforward, at least for the spin-free compounds. With five unpaired $3d$ electrons the ground state is $^6A_1(^6S)$, and this is well-isolated from the lowest-lying excited states. Spin–orbit coupling, which can connect the ground state with the excited states, is very small. This means that g, the spectroscopic splitting factor, is usually quite close to the free-ion value of 2, that g is isotropic, and that crystal-field splittings of the ground state are much smaller than one Kelvin. Thus, spin-only moments, independent of temperature, are the rule. Spin–lattice relaxation times are quite long, which in turn permits EPR spectra to be observable even at room temperature. Furthermore, since this is an odd electron (Kramers) ion, EPR is always detected even if the zero-field splittings should be large. All these generalities for the ferric ion are applicable to the compounds reviewed here.

Two EPR studies have been reported on materials in this series, but they both were on iron(III) doped into the same substance, $(NH_4)_2[InCl_5(H_2O)]$ [15,16]. The results of these studies are similar, with g being nearly isotropic at 2.01 and the zero-field splitting parameter D/k_B being about 0.1–0.25 K. There is also a small rhombic distortion which is nearly 20% of the axial

term. These crystal field splittings are too small to have an observable effect on the bulk magnetic properties which are the subject of this article.

D. MAGNETIC ORDERING

The major interest in these compounds concerns the nature of the spontaneous magnetic ordering which they undergo as they are cooled. The chloride and bromide compounds span ordering temperatures, T_c, from 6.54 to 22.9 K [1,17,18]. These relatively high transition temperatures may be compared with those for such other hydrated halides as $Cs_2CrCl_5 \cdot 4\ H_2O$ ($T_c = 0.185$ K; ref. 19) or $Cs_2MnCl_4 \cdot 2\ H_2O$ ($T_c = 1.8$ K; ref. 20). These substances all exhibit weak anisotropy, and are therefore good examples of the Heisenberg magnetic model [21,22]. This is a model for isotropic magnetic interaction usually described by the Hamiltonian $\mathcal{H} = -2J\Sigma\vec{S}_i \cdot \vec{S}_j$. The indices i and j run over all the lattice sites, though in practice nearest-neighbor interactions are generally the most important. The strength of the interaction is measured by J, the exchange constant, which has units of energy. A negative sign for J means that the interaction is antiferromagnetic in nature. The only fluoride of similar structure which has as yet been examined, $K_2[FeF_5(H_2O)]$, undergoes long-range order at 0.80 K [23]. The behavior of the fluoride compound differs substantially from that of the others and will therefore be discussed separately. General introductions to the subject of magnetic ordering may be found in refs. 21 and 22.

The cesium chloride compound is perhaps the member of this class of compounds that has been most thoroughly studied. Its susceptibility [1] is displayed in Fig. 2, three data sets, measured along each of the crystallographic directions being shown. Above the maximum which occurs at about 7 K, the data sets are coincident, within experimental error. This is a graphic illustration of what is meant by the term magnetic isotropy, and the kind of behavior to which we assign the name, Heisenberg magnetic model compound. The same data are plotted with different (reduced) scales in Fig. 3 in order to facilitate comparison with theory. The fit illustrated [24] is to a high-temperature-series expansion for the susceptibility of the simple-cubic, spin $S = 5/2$, Heisenberg antiferromagnet. The exchange constant, which is the fitting parameter, in this case is $J/k_B = -0.310$ K; any discrepancy between theory and experiment is due to the fact that some lattice anisotropy exists in the material since the superexchange pathways are not those which would correspond to an ideal simple cubic (sc) model. As the temperature is decreased, long range order sets in and the susceptibility behaves like that of any normal antiferromagnet, with the susceptibility parallel to the axis of preferred spin alignment dropping to zero at low temperatures. The a-axis is the easy axis, as it is with all the chloride and bromide analogs.

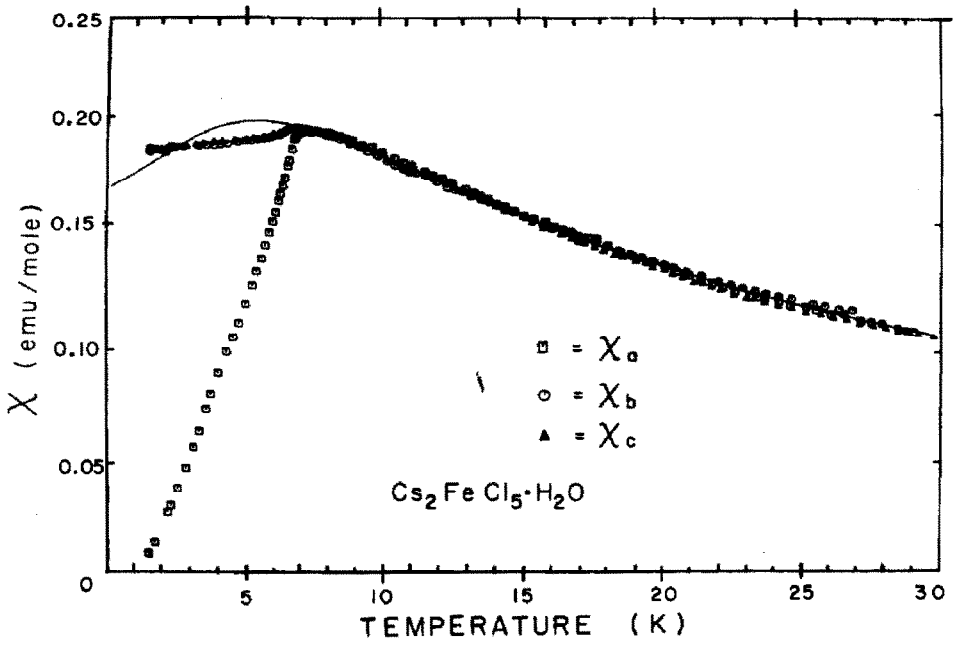

Fig. 2. Magnetic susceptibility of $Cs_2[FeCl_5(H_2O)]$ measured along the three crystal axes. From ref. 1.

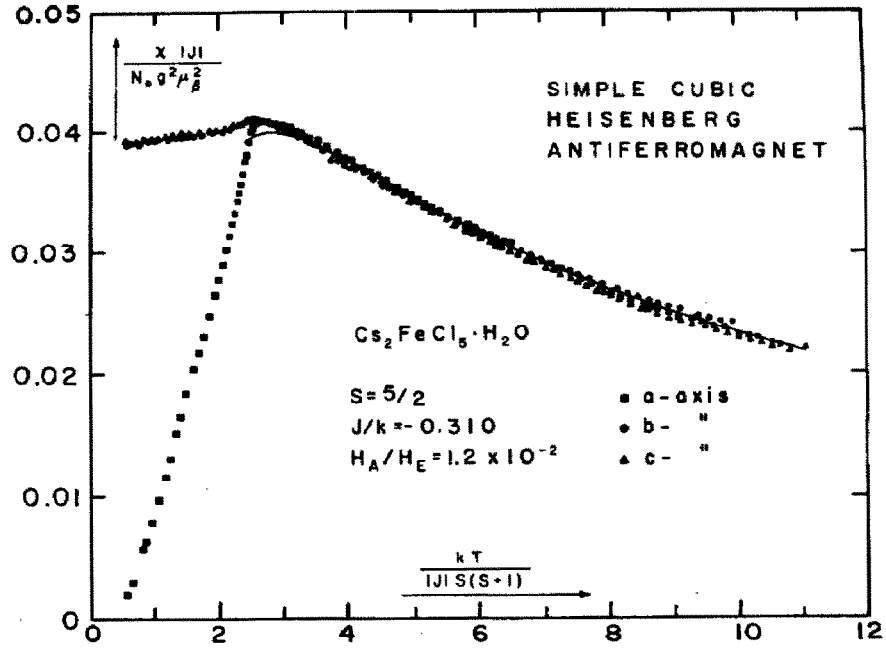

Fig. 3. The magnetic susceptibilities of Fig. 2, plotted on reduced scales in order to emphasize the isotropy above the critical temperature. The solid curve is the calculated high temperature series expansion. From ref. 23.

These data have been reanalyzed together with accurate heat capacity data [13]. Using extrapolation techniques of the high temperature series based on Pade approximants, the antiferromagnetic critical temperature (T_c), height (χ_{max}) and position on the temperature axis $T(\chi_{max})$ of the susceptibility maximum for the Heisenberg antiferromagnet with $S = 5/2$ on the simple cubic and body-centered cubic lattices were calculated. The results for the sc lattice are as follows:

$$k_B T_c/|J|S(S+1) = 2.84$$

$$k_B T(\chi_{max})/|J|S(S+1) = 3.07$$

$$\chi_{max}|J|/Ng^2\mu_B^2 = 0.0394.$$

Using these theoretical predictions and the experimental values $T_c = 6.43$ K, $T(\chi_{max}) = 7.20$ K and $\chi_{max} = 0.207$ emu mol^{-1}, an average value of $|J|/k_B = 0.275$ K fits the three predictions for $Cs_2[FeCl_5(H_2O)]$, within the limitations of the model. Susceptibility data in the ordered region have also been analyzed by using conventional free-spin wave theory for an sc Heisenberg antiferromagnet with $S = 5/2$ and anisotropy constant $\alpha = 1.2 \times 10^{-2}$. The fit provided values of $J/k_B = -0.31$ K and $J/k_B = -0.29$ K when data from the perpendicular and parallel susceptibilities, respectively, were used.

The specific heat of $Cs_2[FeCl_5(H_2O)]$ has also been measured [1,13], and is illustrated in Fig. 4. The transition temperature is a relatively low one, 6.54 K. This is advantageous because specific heat measurements are an integral part of any magnetic investigation, and the magnetic contribution to the specific heat is the more easily determined the lower the magnetic transition temperature. The lattice contribution was evaluated empirically in this case. The resulting data have been analyzed in detail [13]. The data and the analysis are consistent with a three-dimensional character of the magnetic lattice, since a significant one-dimensional character in the magnetic ordering would appear as a broad Schottky-type anomaly in the heat capacity curve. Moreover, the entropy parameter $(S_\infty - S_c)/R$ is found to have the value 0.42 for infinite spin S on a simple-cubic lattice (there are no calculated values for $S = 5/2$, but the values should be close), and the experimental value is 0.4. The agreement is good in view of the various approximations and is one of the strongest arguments in favor of the three-dimensional nature of the ordering of $Cs_2[FeCl_5(H_2O)]$. In the evaluation of the exchange interaction, spin–wave theory has been used on the low temperature side and high temperature series on the higher temperature side of the peak. The values of $J/k_B = -0.27$ K in the ordered region and $|J|/k_B = 0.26$ K in the paramagnetic one give a satisfactory agreement with the experimental points when a simple cubic Heisenberg antiferromagnetic model is used.

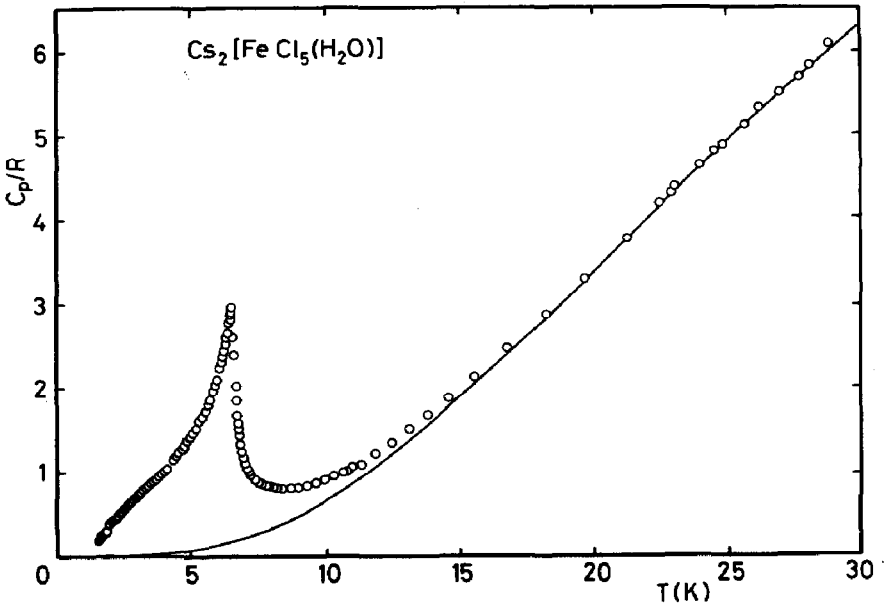

Fig. 4. Specific heat of $Cs_2[FeCl_5(H_2O)]$. The points are experimental and the curve is the estimated lattice contribution. From ref. 13.

The susceptibility of $Rb_2[FeCl_5(H_2O)]$ has been measured twice [1,4,18], as has the specific heat (Fig. 5) [14,18]. The magnetic contribution was evaluated empirically. The susceptibility data were initially interpreted in terms of a one-dimensional chain with an important molecular field (interchain) correction. Both sets of data have since been analyzed as follows in terms of magnetic lattice dimensionality crossover theory [14].

In the case of non-negligible interchain interaction we must consider the Heisenberg hamiltonian with two different types of neighbors

$$\mathcal{H} = -2J\Sigma^{(d)}\vec{S}_i \cdot \vec{S}_j - 2J'\Sigma^{(3-d)}\vec{S}_i \cdot \vec{S}_j$$

where the first summation runs over nearest neighbors in d lattice directions and the second is along the other $3-d$ directions. In the present case, the analysis of superexchange paths suggests $d=1$. The only high temperature series expansions calculated for this model are in the classical limit of $S=\infty$. Since it is physically significant to use such expansions to fit the data for an $S=5/2$ system in the paramagnetic region, it has been analyzed recently for several values of $R=(J'/J)$ using Padé approximants [14,25]. The case of a lattice dimensionality crossover from a linear chain system to a simple cubic lattice was studied by calculating the values of the reduced critical temperature, $k_B T_c/|J|$, the reduced value of the susceptibility maximum, $\chi_{max}|J|/Ng^2\mu_B^2$, and the reduced temperature at which the maximum in the susceptibility occurs, $k_B T(\chi_{max})/|J|$ for different values and signs of

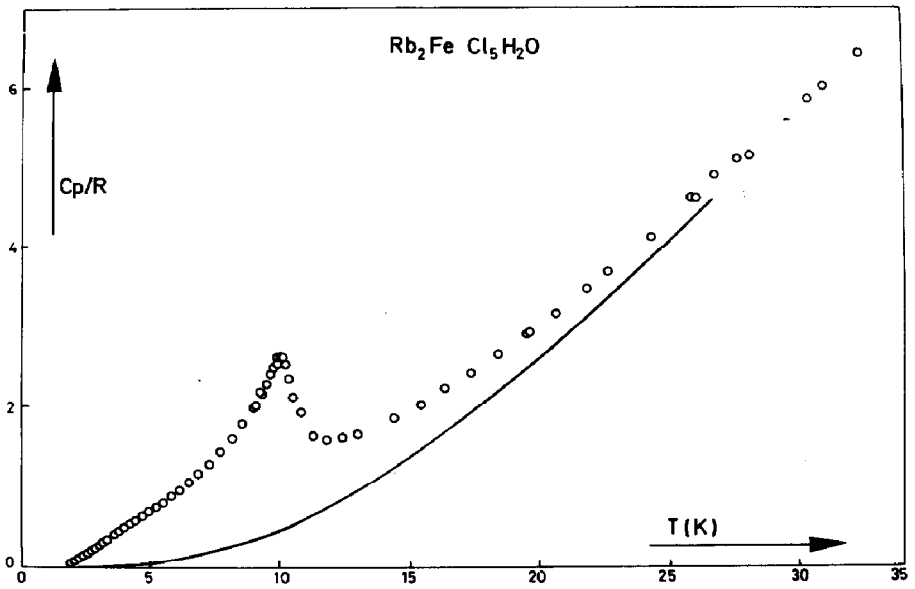

Fig. 5. Specific heat of $Rb_2[FeCl_5(H_2O)]$. The points are the experimental data, and the curve is the estimated lattice contribution. From ref. 14.

J and J'. By substituting the experimental values for $Rb_2[FeCl_5(H_2O)]$ of $T_c = 10.0$ K, $T(\chi_{max}) = 12.5$ K and $\chi_{max} = 0.088$ emu mol^{-1}, a reasonably consistent fit is obtained for $R = 0.15$ with the average value $J/k_B = -1.45$ K when the results are scaled to the true spin of $S = 5/2$. The smaller the value of R that is found, the more a material resembles a magnetic linear chain. In the present case, while there is some low-dimensional character the material cannot be considered, even to a first approximation, to be a linear chain. However, the above results indicate that the system starts ordering antiferromagnetically along one direction and then develops three-dimensional ordering, again through antiferromagnetic interactions. The above values were confirmed by substituting them into the theoretical predictions of the susceptibility and specific heat and comparing the results to the experimental data over the whole temperature range. Furthermore, spin wave theory was developed for the present case of magnetic lattice dimensionality crossover by allowing antiferromagnetic linear chains to interact antiferromagnetically with each other for different degrees of interaction ratio R and strength of the intra-chain interaction, J [14]. No discrepancies were found when the experimental results were compared with theoretical predictions for the parallel and perpendicular susceptibilities and the specific heat ($T < T_c$) calculated for $R = 0.15$ and $J/k_B = -1.45$ K, the anisotropy parameter being $\alpha = 3.4 \times 10^{-3}$ [26].

The potassium salt, $K_2[FeCl_5(H_2O)]$, with a transition temperature of 14.06 K has one of the highest T_c's ever reported for a hydrated transition

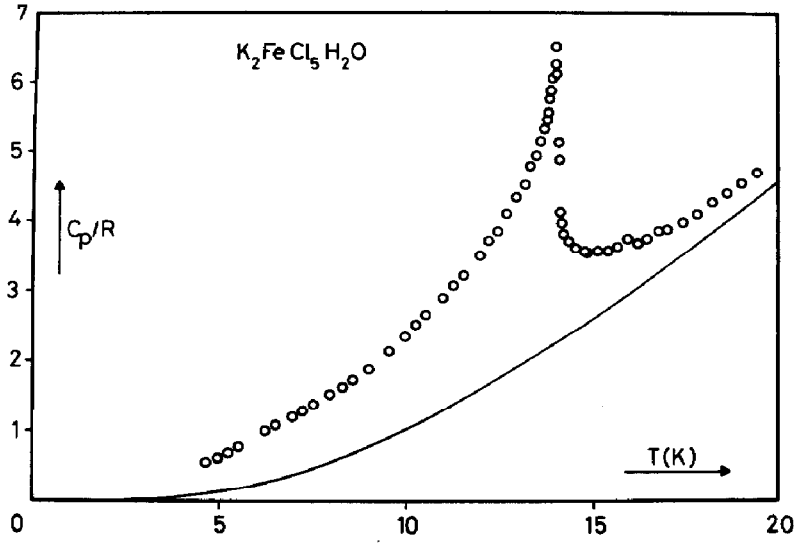

Fig. 6. Specific heat of $K_2[FeCl_5(H_2O)]$. The solid curve represents the estimated lattice specific heat contribution. From ref. 12.

metal chloride double salt. This is clearly indicative of unusually extensive exchange interactions. The susceptibility behavior resembles that of $Cs_2[FeCl_5(H_2O)]$, except that the data are shifted to higher temperatures, consistent with the higher ordering temperature. The specific heat, illustrated in Fig. 6 [12], exhibits the usual λ-feature, but the relatively high transition temperature makes difficult the separation of the lattice and magnetic contributions. Just the same, it has been estimated that about 85% of the total expected magnetic entropy has already been gained below the transition temperature. This is consistent with the primarily three-dimensional character of the magnetic lattice. The data have been reanalyzed [14] according to the same model used to analyze $Rb_2[FeCl_5(H_2O)]$, using the characteristic experimental values $T_c = 14.06$ K, $T(\chi_{max}) = 16.0$ K and $\chi_{max} = 0.068$ emu mol^{-1}. An exchange constant $J/k_B = -1.44$ K ($S = 5/2$) was estimated, with a crossover parameter $R = 0.20$–0.35.

The ammonium compound, $(NH_4)_2[FeCl_5(H_2O)]$, presents special problems. It exhibits two closely-spaced λ-anomalies in the specific heat [12], at 6.87 and 7.25 K. It appears to have a great deal of short range magnetic order, and it does not behave like a normal two-sublattice antiferromagnet in that it does not exhibit the usual type of easy-axis behavior. No data-set in the susceptibility measurements approaches zero value at low temperatures. Most likely the peak at 7.25 K marks the transition of the system to long-range magnetic order while the anomaly at 6.87 K can be associated with a spontaneous reorientation of the antiferromagnetic axis. Although spin-reorientations in the ordered state are generally ascribed to the presence

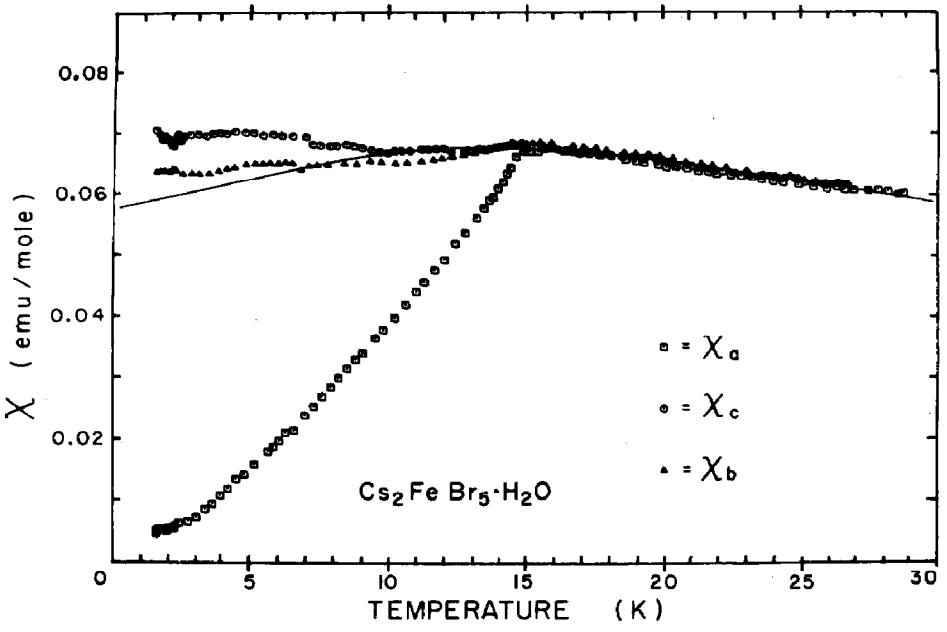

Fig. 7. Magnetic susceptibility of $Cs_2[FeBr_5(H_2O)]$ along the three orthogonal crystallographic axes. The points are experimental and the solid curve represents a tentative fit using molecular field theory. From ref. 17.

of significant spin anisotropy, they have also been found in several other isotropic compounds since reorientations can also depend on the form of the spin–spin interactions. In fact, preliminary Mössbauer studies of $(NH_4)_2[FeCl_5(H_2O)]$ show two distinct sublattice magnetization curves [27]. On the other hand, the ammonium counterion is the one cation in this series of compounds that is able to undergo rotational transitions as the sample is cooled and it has been shown that the isomorphous $(NH_4)_2[InCl_5(H_2O)]$ undergoes a crystal phase transition at 100 K [28,29]. If an analogous transition takes place in the iron compound, then the room temperature crystal structure would differ from that of the compound at the temperatures where magnetic ordering occurs. In the absence of detailed information on this transition, it is fruitless to discuss this substance further at this time.

Two bromides have also been investigated [17,18], $Cs_2[FeBr_5(H_2O)]$ and $Rb_2[FeBr_5(H_2O)]$. They have high ordering temperatures, 14.2 and 22.9 K, respectively. Thus the available susceptibility data concentrate on the ordered region, simply because the investigators could not measure at high-enough temperatures! As shown from the susceptibility plot for $Cs_2[FeBr_5(H_2O)]$ illustrated in Fig. 7, the behavior is typical, with the exception of the anisotropy observed between the two perpendicular susceptibilities in the ordered region. The *a*-axis is the easy axis for both compounds; it is remarkable that the *a*-axis remains the preferred axis of spin alignment

TABLE 2

Magnetic properties of $A_2[FeX_5(H_2O)]$

A, X	Cs, Cl	NH_4, Cl	Rb, Cl	K, Cl	Cs, Br	Rb, Br
$T_c(0)$(K)	6.54	7.25, 6.87	10.00	14.06	14.1 12.9	22.90
T_b (K)	6.3		9.75	13.6		
H_b (kOe)	14.7		17.8	34.1		
$H_{SF}(0)$ (kOe)	11.5		14.3	27		
H_A (kOe)	0.88		0.59	1.7		
H_E (kOe)	75.9		172.4	199.4		
α	1.2×10^{-2}		3.4×10^{-3}	8.5×10^{-3}		

throughout the series of compounds. Preliminary specific heat data on $Cs_2[FeBr_5(H_2O)]$ suggest that there are two λ-like transitions, at 14.1 and 12.9 K. These results require confirmation, but are suggestive of a spin-reorientation transition at the lower temperature. The anisotropy does not appear to occur until the temperature is lowered to about 13 K. Susceptibility data at higher temperatures would also be useful.

There are no discontinuous changes in the electronic spectra as the critical temperature is crossed [2]. The magnetic phase transitions are thus not likely to be accompanied by drastic structural changes. Any exchange-induced intensity mechanisms make a small if not negligible contribution.

The transition temperatures of the different $A_2[FeX_5(H_2O)]$ compounds are collected in Table 2. For a given alkali ion, T_c for a bromide compound is always higher than that of the chloride analogue. This is a common phenomenon [1]. Note also the general increase in transition temperature with decreasing radius of the alkali ion.

E. THE FLUORIDE, $K_2[FeF_5(H_2O)]$

This compound is considered separately from the others because it is the lone $A_2[FeX_5(H_2O)]$ compound which clearly exhibits what might be called classical antiferromagnetic linear chain behavior [23]. It shows the characteristic broad maximum in the susceptibility which identifies quasi-one-dimensional systems; the specific heat, which should likewise show a broad maximum, has not yet been measured. This difference in behavior from the other systems described follows from the structural features of this monoclinic compound. Though there are still discrete octahedra in the crystal lattice, they are connected by hydrogen bonds; it is well-known that fluoride ion can hydrogen-bond more strongly than either chloride or bromide. Thus, although fluoride usually does not provide as efficient an exchange path as chloride or bromide, in this case strong hydrogen bonding provides a more

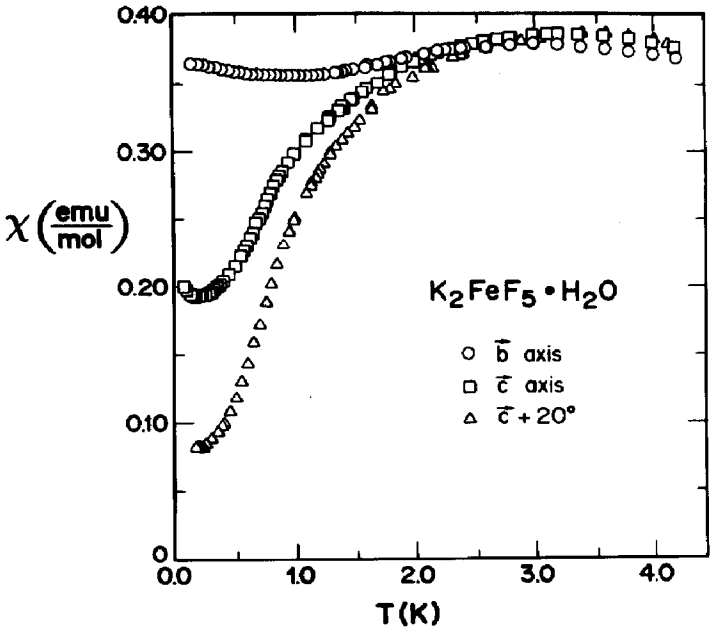

Fig. 8. Zero field magnetic susceptibilities of $K_2[FeF_5(H_2O)]$ below 4.2 K. The *b*-axis is the hard one, and the others *c* and $c+20°$ form angles of 50° and 30° respectively with the easy axis of the magnetization. From ref. 23.

directional character to the exchange. The material indeed appears to provide one of the first good examples of a one-dimensional antiferromagnet of iron(III).

The three susceptibility data sets exhibit broad maxima at about 3.4 K; a portion of the data is illustrated in Fig. 8. The system undergoes long range antiferromagnetic ordering at $T_c = 0.80$ K, with the preferred direction of spin alignment in the *ac* plane. Using the available high-temperature-series expansion and Padé approximant techniques the susceptibility can be calculated down to the temperature of the maximum, $T(\chi_{max})$. The experimental results from 280 K down to 10 K can be fitted to these theoretical values with a Landé *g*-factor, typical for the ferric ion, of 1.97 and an exchange constant of $J/k_B = -0.40$ K. At temperatures below 10 K the data points increasingly deviate to values higher than the theoretical ones; at low temperatures, interchain interactions become important and long-range magnetic order occurs.

A consideration of the transition temperature $T_c = 0.80$ K following the calculations of Oguchi [30] yields a value for $R = |J'/J| = 1.4 \times 10^{-2}$, where J' represents the interchain interactions. The low-dimensional magnetic character is not ideal. Weak interactions of the metal ions with their next-nearest-neighbors become important below 10 K and the correlation between magnetic moments on different chains produces a lattice dimen-

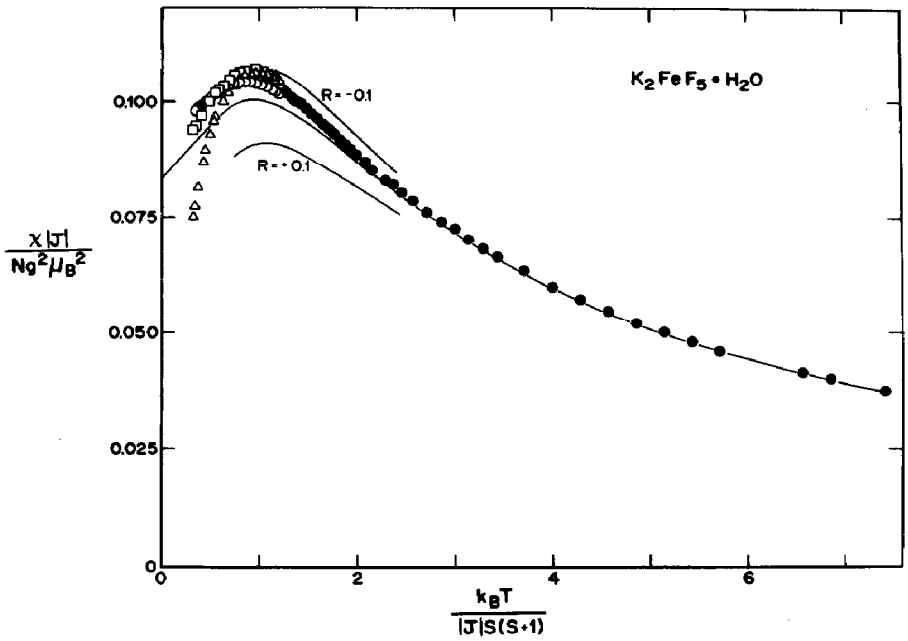

Fig. 9. Zero field susceptibilities of $K_2[FeF_5(H_2O)]$ in the paramagnetic region. The solid symbols are data points which have been taken on powders, while the open ones represent the measurements in the three principal directions. The continuous line is the solution for the classical Heisenberg linear chain and the values of R give the calculations for three-dimensional crossover with ferro- and antiferromagnetic interchain constants. From ref. 23.

sionality crossover from a linear-chain system to an anisotropic simple cubic lattice.

From the experimental measurements the average susceptibility in the three main directions yields

$$\frac{\chi_{max}|J|}{Ng^2\mu_B^2} = 0.105, \text{ and } \frac{k_B T(\chi_{max})}{|J|S(S+1)} = 1.00.$$

The fact that the reduced susceptibility is higher than the corresponding one for the pure linear chain antiferromagnet implies the presence of some ferromagnetic interaction. The value of the susceptibility at the maximum is known with precision and it allows one to calculate $R = -0.06 \pm 0.02$, or J' is ferromagnetic. The value of the interchain interaction is low enough for the compound to behave as a good linear chain above the temperature $2T(\chi_{max})$, yet is sufficiently high to allow the observation of the crossover effects in the paramagnetic region and quantitative comparisons with the theory to be made, as depicted in Fig. 9.

F. MAGNETO–STRUCTURAL RELATIONS

The structural and magnetic ordering characteristics for each member of the $A_2[FeX_5(H_2O)]$ series have been reviewed in previous sections. Since

these compounds differ magnetically from each other mainly due to their individual lattice dimensionalities, it seems relevant at this point to consider on a comparative basis their structural properties which, in the end, are the origin of the magnetic differences.

The fluorine compound is the only one which shows well-defined one-dimensional characteristics. The magnetic ions in $K_2[FeF_5(H_2O)]$ are linked through double Fe–F---O–Fe bridges symmetrically centered with Fe–Fe distances of 5.11 Å [7]. The small value of the F---O distance, 2.54 Å, is consistent with strong hydrogen-bond formation. This, together with the greater spatial extension of the oxygen electronic wave functions compared with those of the fluoride ions, gives a preferential direction to the magnetic interaction. This structural feature is illustrated in Fig. 10.

The chloride members of the series each exhibit several superexchange paths connecting each iron with its nearest and next nearest magnetic neighbors. The various paths consist of double bridges of the type Fe–Cl---O–Fe or of the type Fe–Cl---Cl–Fe, or mixed double bridges consisting of one of each of these paths. Since the bond angles and distances vary from

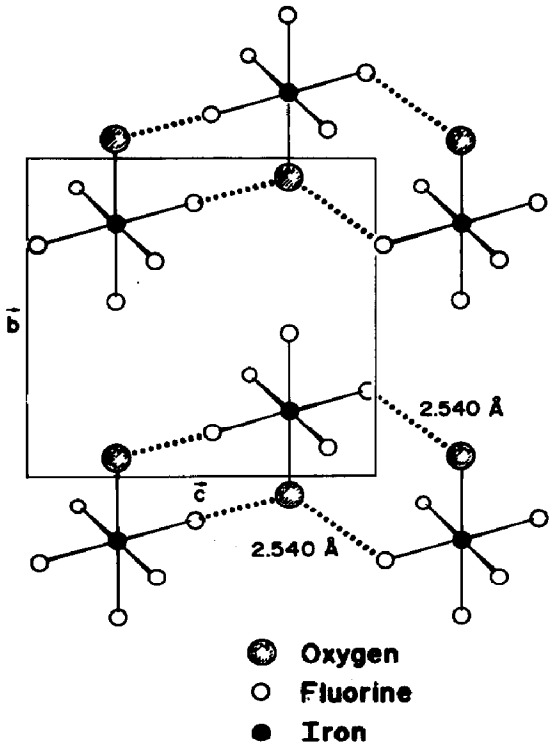

Fig. 10. Hydrogen-bonded chains of metal octahedra in $K_2[FeF_5(H_2O)]$. The dashed lines represent the hydrogen bonds. The unit cell in the *bc* plane is indicated. From ref. 23.

one superexchange path to another, not all those paths are equivalent. It is well-known that the superexchange interactions are sensitive to small variations in the crystal structure, the dependence for singly-bridged paths being of the order of r^{-12}, where r is the internuclear separation [21]. As a consequence, the chloride derivatives are all closer to a three-dimensional behavior than to a linear chain and the analysis of the interaction paths does not allow predictions as to how well any particular compound approximates a three-dimensional model.

A clear example of this uncertainty is provided by $Cs_2[FeCl_5(H_2O)]$. It is possible to distinguish in this compound three principal superexchange paths. The first, labeled with the exchange constant J_1, would go through mixed oxygen–chlorine double bridges forming zig-zag chains parallel to the c-axis. A second interaction, J_2, connects, through double chlorine–chlorine

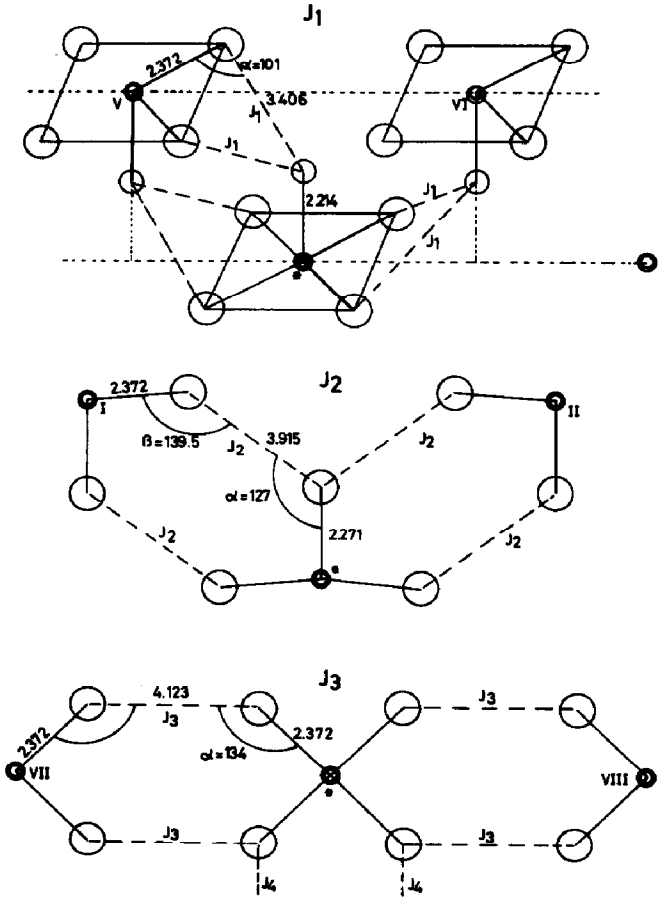

Fig. 11. Superexchange interaction paths for $Cs_2[FeCl_5(H_2O)]$. Only the relevant distances and angles have been written down. In the top diagram, the $FeCl_4$ plane lies in the *ac* plane. From ref. 13.

bridges every iron atom with the four nearest neighbors that have the apical O–Fe–Cl axis inverted with respect to one another. Therefore, this interaction propagates within a layer parallel to the *ac* plane. The last interaction, J_3, connects iron atoms through equatorial chlorines in a direction parallel to the *a*-axis. These paths are shown schematically in Fig. 11. A careful analysis of the structure allows one to order the interactions as $J_1 > J_2 > J_3$ [13], from which a certain amount of lower dimensionality could be expected. However, the nature of the specific heat excludes this possibility. If, on the other hand, J_2 (or J_3) is competitive with J_1, the behavior becomes three-dimensional directly because bonds extend three-dimensionally in the lattice. Another problem arises when one considers the number of magnetic neighbors, z, around every iron ion. If J_3 is negligible, then the effective z is 6 and data should fit to a simple cubic lattice model. As has been shown above, agreement with theory is quite good although not complete. If, on the other hand, $J_1 = J_2 = J_3$, then $z = 8$ and data should fit better to a body-centered cubic model. Such a fit has been made [13] and agreement with theory has been found to be of about the same quality as when the simple cubic lattice is considered. Therefore, it seems certain that the J_3 interaction is not negligible compared with J_2.

In the set of isostructural compounds $A_2[FeCl_5(H_2O)]$ (A = Rb, K and NH_4), one can distinguish up to four inequivalent superexchange paths. Although these paths differ from those described for the cesium compound, they present similar uncertainties for a correlation with magnetic properties. A detailed description is given in ref. 14. The experimental data suggest a degree of lower dimensionality for $Rb_2[FeCl_5(H_2O)]$, while this result is less pronounced with $K_2[FeCl_5(H_2O)]$. The one-dimensional character of $(NH_4)_2[FeCl_5(H_2O)]$ should be somewhat enhanced, relatively.

G. FIELD-DEPENDENT BEHAVIOR

The phenomenon of spin-flop [22,31] occurs when antiferromagnets with small anisotropy such as these are subjected to an applied magnetic field. The field must be applied parallel to the easy axis or axis of preferred spin alignment, and the system must be below the transition temperature, $T_c(H_a = 0) \equiv T_c(0)$. There is a boundary between the paramagnetic and antiferromagnetic phases which is field-dependent, but there is also another phase, the spin-flop phase. This is attained when the field is applied in the antiferromagnetic state; the spins are found to flop perpendicular to the easy axis when a certain critical field is reached. The AF → SF transition is discontinuous or first-order, while the AF–P boundary is a second-order or continuous one. There is a discontinuity in the magnetization on crossing the AF–SF phase boundary; a peak in the susceptibility is observed at constant

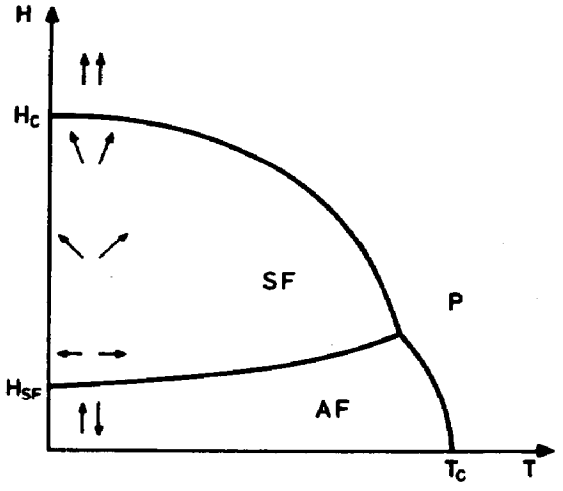

Fig. 12. Schematic phase diagram for a typical antiferromagnet with small anisotropy with the external field applied parallel to the preferred axis of spin alignment.

temperature as the applied field is increased. As the field reaches a high enough value, there is finally a transition from the spin-flop state to the paramagnetic one. The three phases meet at a point, called the bicritical point, at temperature T_b and applied field H_b. A hypothetical phase diagram is illustrated in Fig. 12.

The phase diagrams for $Cs_2[FeCl_5(H_2O)]$, $Rb_2[FeCl_5(H_2O)]$ and $K_2[FeCl_5(H_2O)]$ have all been determined and are illustrated in Figs. 13–15. The diagrams are quite similar to one another, as well as to the schematic diagram in Fig. 11. The differences are of course due to the different magnetic parameters that describe each system. Indeed, several of the magnetic parameters can be evaluated independently and with greater accuracy from the field-dependent properties than from fitting the zero-field susceptibilities to a model, for example. An anisotropy field, H_A, can be defined as the sum of all those factors which contribute to the lack of the ideal isotropic interactions in a magnetic system. The most important such factors are single-ion or crystal-field anisotropy and dipole–dipole interactions; if zero-field splitting alone were to contribute, then $g\mu_B H_A = 2|D|(S - \frac{1}{2})$, where S is the spin of the magnetic ion. From the discussion above, one does not expect H_A to be large for the $A_2[FeX_5(H_2O)]$ compounds. One may also define the exchange field, H_E, which is given by $g\mu_B H_E = 2z|J|S$, where J is the exchange constant and z is the magnetic coordination number. The ratio $\alpha = H_A/H_E$ is a useful relative measure of the ideality of the isotropic nature of the exchange interaction. One can also show by molecular field theory that $H_{SF}(0)$, the value of the antiferromagnetic-to-

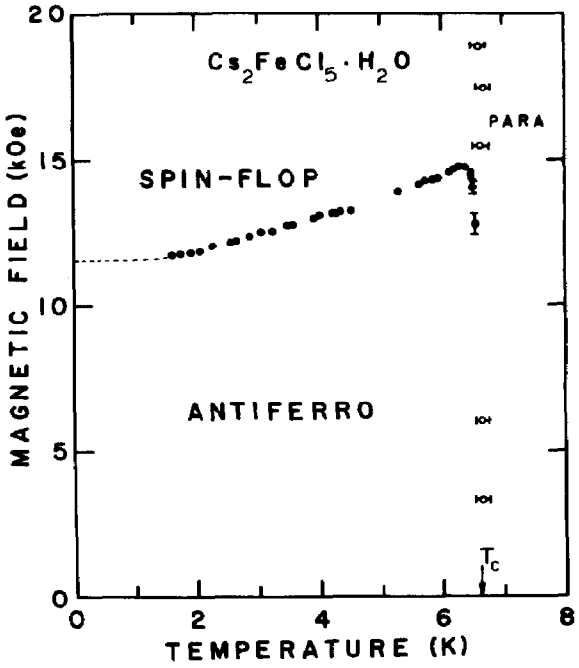

Fig. 13. Magnetic phase diagram of $Cs_2[FeCl_5(H_2O)]$. From ref. 24.

spin-flop transition field extrapolated to 0 K, is given by

$$H_{SF}(0) = \left[2H_E H_A - H_A^2\right]^{1/2}$$

and that $H_c(0)$, the field of the spin-flop-to-paramagnetic transition ex-

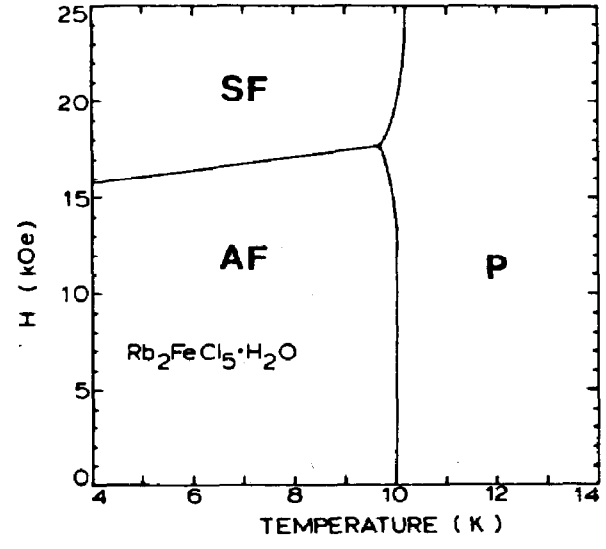

Fig. 14. Magnetic phase boundaries of $Rb_2[FeCl_5(H_2O)]$. From ref. 4.

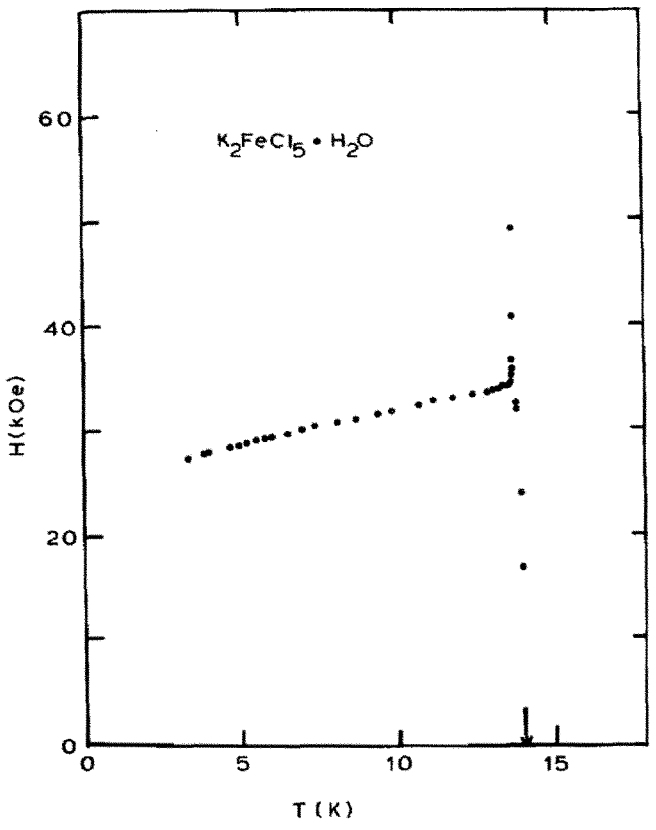

Fig. 15. Magnetic phase diagram of $K_2[FeCl_5(H_2O)]$. From ref. 26.

trapolated to 0 K, equals $2H_E - H_A$. Thus observation to low temperatures of these boundaries allows a determination of several important quantities. Clearly, the higher the value of $T_c(0)$, the greater the exchange field will be and there will be a consequent increase in both $H_{SF}(0)$ and $H_c(0)$.

The first of the $A_2[FeX_5(H_2O)]$ series of materials that was examined in this fashion was [24] $Cs_2[FeCl_5(H_2O)]$. The bicritical point was found at $T_b = 6.3$ K and $H_b = 14.7$ kOe. Unfortunately, $H_c(0)$ is estimated to be about 150 kOe for $Cs_2[FeCl_5(H_2O)]$, a value difficult to reach. In cases such as this, one can also make use of the relationship that the zero-field susceptibility perpendicular to the easy axis extrapolated to 0 K takes the value $\chi_\perp(0) = 2M_s/(2H_E + H_A)$, where $M_s = Ng\mu_B S/2$ is the saturation magnetization of one antiferromagnetic sublattice. Since $\chi_\perp(0)$ is relatively easy to measure, this relationship in combination with that for $H_{SF}(0)$ can be used to determine H_A and H_E. The anisotropy field was estimated as $H_A = 0.88$ kOe and the exchange field $H_E = 75.9$ kOe. The parameter α is then 1.2×10^{-2}. One interesting feature is that the antiferromagnetic-paramagnetic phase boundary is quite vertical $[T_b/T_c(0) = 0.96]$ as has been

observed in several other low-anisotropy antiferromagnets. The main source of anisotropy is probably due to the orthorhombic structure of the compound.

The phase diagram of $Rb_2[FeCl_5(H_2O)]$ is quite similar [4,26]. The bicritical point is found at 9.75 K and 17.8 kOe. With an H_A of only 0.6 kOe and an H_E increased to 172 kOe, the anisotropy appears to be even less in this compound; α is 3.4×10^{-3}. Therefore this salt is also a good example of the Heisenberg magnetic model system.

The final compound in this series whose phase diagram has been determined is $K_2[FeCl_5(H_2O)]$ [26]. It is shown in Fig. 15, where it will be seen that it resembles those of the other systems closely. Note once again the steep verticality of the boundary separating the antiferromagnetic and paramagnetic phases. The bicritical point occurs at 13.6 K and 34.1 kOe, and the spin-flop field extrapolated to zero temperature is about 27 kOe. One can therefore calculate an anisotropy field of 1.7 kOe and an exchange field of 199 kOe. The anisotropy parameter α is 8.5×10^{-3} and the exchange constant that results from the data analysis is $zJ/k_B = -5.4$ K, which compares rather well with the value $2J_z + 4J_{xy} = -4.90$ K calculated from the reported values of J_z and J_{xy} in the analysis of the susceptibility and specific heat for $R = 0.35$.

The phase diagram of $(Rb_{0.25}K_{0.75})_2[FeCl_5(H_2O)]$ has recently been determined and the boundaries are located between those of the pure rubidium and potassium systems (A. Paduan Filho, private communication).

The anisotropy field appears to be anomalously small in all of these crystals. Perhaps the dipole–dipole interactions, which should be small, act in opposition to the other contributors to the anisotropy field. The results described above are collected in Table 2. The iron systems are compared in Table 3 with several other compounds which are good examples of the

TABLE 3

Antiferromagnetic Heisenberg 3-D magnetic model systems

	Crystal lattice	S	T_c (K)	H_A/H_E
$CuCl_2 \cdot 2\,H_2O$	Orthorhombic	1/2	4.36	10^{-2}–10^{-3}
$KNiF_3$	Cubic (perovskite)	1	246	Small
Cr_2O_3	Rhombohedral	3/2	307.0	2.9×10^{-4}
$RbMnF_3$	Cubic (perovskite)	5/2	83.0	5×10^{-6}
MnF_2	Tetragonal (rutile)	5/2	67.33	1.6×10^{-2}
$Cs_2FeCl_5 \cdot H_2O$	Orthorhombic	5/2	6.54	1.2×10^{-2}
$Rb_2FeCl_5 \cdot H_2O$	Orthorhombic	5/2	10.00	3.4×10^{-3}
$K_2FeCl_5 \cdot H_2O$	Orthorhombic	5/2	14.06	8.5×10^{-3}

Heisenberg magnetic model. Among the spin $S = 5/2$ systems, it will be seen that the temperature of the critical point of the $A_2[FeX_5(H_2O)]$ systems is more convenient for future studies of, for example, critical phenomena.

H. PRESSURE-DEPENDENT PROPERTIES

Studies of magnetic compounds under pressure can yield valuable information about the dependence of exchange interactions upon interatomic distance. One of the crystals of interest in this article, $K_2[FeCl_5(H_2O)]$, has been subjected to hydrostatic pressures of up to 10 kbar [32,33]. In particular, the temperature dependence of the spin-flop field was studied. The data were analyzed in terms of the orthorhombic symmetry of the crystal, and it was found, as expected, that interactions of an ion with its neighboring spins are antiferromagnetic. However, interactions with second neighbors were found to be ferromagnetic and comparable in magnitude to those with first neighbors. In addition, a considerable anisotropy in the exchange interactions from one direction to another was observed.

The above conclusions follow from data such as are presented in Fig. 16. Isotherms of the spin-flop field vs. applied pressure are plotted in this figure. Note the sharp drop in H_{SF} below 1 kbar and then the change in slope at higher pressures. Note also the fact that dH_{SF}/dP is negative, and the slope of the curves appears to be independent of temperature. All the transitions resemble spin-flop transitions. There is also a rather small dependence of T_c upon pressure, with the transition temperature increasing by only about 0.2 K for about 8 kbar. It is not clear why there is a change in the slope in Fig. 15 at about 1 kbar, but it is possible that this behavior may be due to a

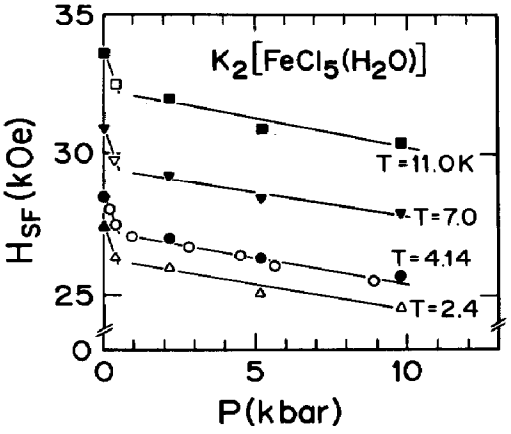

Fig. 16. Pressure dependence of the spin-flop field of $K_2[FeCl_5(H_2O)]$ at a series of constant temperatures. From ref. 33.

pressure-induced change of the intermediate and hard magnetic axes, i.e., a change in the local anisotropies.

A consideration of the variation of the lattice parameters with pressure is not by itself sufficient to explain the behavior of T_c and H_{SF} with pressure. For example, $Rb_2[FeCl_5(H_2O)]$ possesses a unit cell which is a few percent larger than that of $K_2[FeCl_5(H_2O)]$, while $H_{SF}(0)$ and T_c for this first compound are, respectively, one-half and two-thirds of the corresponding values for the potassium isomorph. Thus, on the basis of lattice parameter considerations alone [33], one would expect an increase in H_{SF} and T_c for $P > 1$ atm for $K_2[FeCl_5(H_2O)]$. On the contrary, H_{SF} decreases with pressure, while T_c shows a small increase. This shows that pressure modifies the superexchange interactions in these materials in a rather subtle fashion. On the other hand, if the effect of pressure is to reduce the distortion of the octahedron which surrounds the iron ion, then it is probable that the anisotropy of the material should decrease with increasing pressure.

I. CONCLUSIONS

Compounds of the general formula $A_2[FeX_5(H_2O)]$ form one of the largest series of isomorphous antiferromagnets extant. They are orthorhombic and the *a*-axis is always the easy axis. They furnish a number of good examples of compounds which follow the Heisenberg magnetic model, but the magnetic coordination numbers are large and, in some cases, uncertain. There remain many experiments to be done on these salts. The alkali and halide ions are generally suitable for nuclear resonance experiments, which can provide more information about the spin structures. A large number of Mössbauer experiments remain to be carried out. The two peaks in the zero-field specific heat of $(NH_4)_2[FeCl_5(H_2O)]$ and $Cs_2[FeBr_5(H_2O)]$ show that these compounds may undergo a spin reorientation, and thus their magnetic phase diagrams should be determined. Unfortunately, rather large fields will be required. Several of the compounds are probably suitable for critical point studies of spin $S = 5/2$ systems. The structural phase transitions which the ammonium salts appear to undergo need to be examined.

One of the most significant problems yet to be worked on with these salts concerns the properties of mixed and diluted compounds. As was pointed out above, the indium and iron salts are isomorphous and since the indium materials are diamagnetic, it would be interesting to determine the phase diagram of the mixed systems. The transition temperatures will decrease with dilution, but the detailed behavior needs to be mapped out. Mixed systems in which different relative concentrations of either the alkali metal ions or the halide ions are prepared are also of current interest.

Finally, analogs of the $A_2[FeX_5(H_2O)]$ series of molecules in which the iron is replaced by some other magnetic ion remain to be studied. The chromium(III) analog, while an interesting system [19], is nevertheless of different stoichiometry, $Cs_2CrCl_5 \cdot 4\ H_2O$, and structure, and therefore is not relevant here. Reference has already been made to $(NH_4)_2[MoBr_5(H_2O)]$, which is currently under investigation [35]. Ruthenium(III) falls beneath iron(III) in the periodic chart, and does indeed form several salts of stoichiometry $A_2[RuCl_5(H_2O)]$. Reference was made earlier to the crystal structure of the cesium salt. Ruthenium(III), while a d^5 ion, is always spin-paired and therefore a spin $S = 1/2$ ion [22]. The cesium salt orders at 0.58 K, the rubidium salt at 2.5 K, and the potassium salt at about 4 K [36]. Studies on these and related materials are continuing.

ACKNOWLEDGMENTS

The research in Chicago has been supported by a succession of grants from the Solid State Chemistry program of the Division of Materials Research of the National Science Foundation, while the research in Zaragoza has been funded by the Comision Asesora de Investigacion Cientifica y Tecnica. The authors thank all their colleagues and collaborators for their efforts in this work. We especially thank Ramon Burriel, Rafael Navarro, Armando Paduan Filho, Charles J. O'Connor and Hans van Duyneveldt for their comments on the manuscript.

REFERENCES

1 R.L. Carlin, S.N. Bhatia and C.J. O'Connor, J. Am. Chem. Soc., 99 (1977) 7728.
2 U. Kambli and H.U. Güdel, Inorg. Chem., 21 (1982) 1270.
3 W.E. Hatfield, R.C. Fay, C.E. Pfluger and T.S. Piper, J. Am. Chem. Soc., 85 (1963) 265.
4 C.J. O'Connor, B.S. Deaver, Jr. and E. Sinn, J. Chem. Phys., 70 (1979) 5161.
5 J.E. Greedan, D.C. Hewitt, R. Faggiani and I.D. Brown, Acta Crystallogr. Sect. B, 36 (1980) 1927.
6 T.E. Hopkins, A. Zalkin, D.H. Templeton and M.G. Adamson, Inorg. Chem., 5 (1966) 1431.
7 A.J. Edwards, J. Chem. Soc. Dalton Trans., (1972) 816.
8 I. Søtofte and K. Nielsen, Acta Chem. Scand. Ser. A, 35 (1981) 821.
9 B.N. Figgis, C.L. Raston, R.P. Sharma and A.H. White, Aust. J. Chem., 31 (1978) 2717.
10 J.P. Wignacourt, G. Mairesse and P. Barbier, Cryst. Struct. Commun., 5 (1976) 293.
11 R.G. Cavell and J.W. Quail, Inorg. Chem., 22 (1983) 2597.
12 J.N. McElearney and S. Merchant, Inorg. Chem., 17 (1978) 1207.
13 J.A. Puertolas, R. Navarro, F. Palacio, J. Bartolome, D. Gonzalez and R.L. Carlin, Phys. Rev. B, 26 (1982) 395.
14 J.A. Puertolas, R. Navarro, F. Palacio, J. Bartolome, D. Gonzalez and R.L. Carlin, Phys. Rev. B, 31 (1985) 516.
15 G.M. Cole, Jr. and B.B. Garrett, Inorg. Chem., 13 (1974) 2680.

16 S.K. Misra and G.R. Sharp, J. Chem. Phys., 66 (1977) 4172.
17 R.L. Carlin and C.J. O'Connor, Chem. Phys. Lett., 78 (1981) 528.
18 C.J. O'Connor, Thesis, University of Illinois at Chicago, 1976.
19 R.L. Carlin and R. Burriel, Phys. Rev. B, 27 (1983) 3012.
20 T. Smith and S.A. Friedberg, Phys. Rev., 177 (1969) 1012.
21 R.L. Carlin and A.J. van Duyneveldt, Magnetic Properties of Transition Metal Compounds, Springer-Verlag, New York, 1977.
22 R.L. Carlin, Magnetochemistry, Springer-Verlag, in press.
23 R.L. Carlin, R. Burriel, J. Rojo and F. Palacio, Inorg. Chem., 23 (1984) 2213, and to be published.
24 A. Paduan Filho, F. Palacio and R.L. Carlin, J. Phys. (Paris), 39 (1978) L-279.
25 J.A. Puertolas, R. Navarro, F. Palacio, J. Bartolome, D. Gonzalez and R.L. Carlin, J. Mag. Mag. Mat., 31–34 (1983) 1243.
26 F. Palacio, A. Paduan Filho and R.L. Carlin, Phys. Rev. B, 21 (1980) 296.
27 H. LeFever and R.C. Thiel, Kamerlingh Onnes Laboratorium, private communication (1976).
28 S.L. Carr, B.B. Garrett and W.G. Moulton, J. Chem. Phys., 47 (1967) 1170.
29 K. Yamada and A. Weiss, Ber. Bunsenges. Phys. Chem., 87 (1983) 932.
30 T. Oguchi, Phys. Rev., 133 (1964) A1098.
31 R.L. Carlin and A.J. van Duyneveldt, Acc. Chem. Res., 13 (1980) 231.
32 W.A. Ortiz, A. Paduan Filho and F.P. Missell, Phys. Lett. A, 77 (1980) 183.
33 W.A. Ortiz, A. Paduan Filho and F.P. Missell, J. Mag. Mag. Mat., 24 (1981) 67.
34 H.P. Klug, D. Kummer and L. Alexander, J. Am. Chem. Soc., 70 (1948) 3064.
35 J.W. Quail, D.W. Carnegie, Jr. and R.L. Carlin, to be published.
36 R.L. Carlin and R. Burriel, to be published.